

Dalek – a deep-learning based emulator for tardis

WOLFGANG E. KERZENDORF,^{1,2} CHRISTIAN VOGL,³ JOHANNES BUCHNER,⁴ GABRIELLA CONTARDO,⁵ MARC WILLIAMSON,⁶
AND PATRICK VAN DER SMAAT^{7,8}

¹*Department of Physics and Astronomy, Michigan State University, East Lansing, MI 48824, USA*

²*Department of Computational Mathematics, Science, and Engineering, Michigan State University, East Lansing, MI 48824, USA*

³*Max-Planck-Institut für Astrophysik, Karl-Schwarzschild-Str. 1, D-85741 Garching, Germany*

⁴*Max-Planck-Institut für extraterrestrische Physik, Giessenbachstrasse 1, 85748 Garching bei München, Germany*

⁵*Center for Computational Astrophysics, Flatiron Institute, New York, NY, 10010, USA*

⁶*Department of Physics, New York University, New York, NY, 10003, USA*

⁷*Machine Learning Research Lab, Volkswagen AG, Munich, Germany*

⁸*Faculty of Informatics, Eötvös Loránd University, Budapest, Hungary*

Submitted to ApJ

ABSTRACT

Supernova spectral time series contain a wealth of information about the progenitor and explosion process of these energetic events. The modeling of these data requires the exploration of very high dimensional posterior probabilities with expensive radiative transfer codes. Even modest parametrizations of supernovae contain more than ten parameters and a detailed exploration demands at least several million function evaluations. Physically realistic models require at least tens of CPU minutes per evaluation putting a detailed reconstruction of the explosion out of reach of traditional methodology. The advent of widely available libraries for the training of neural networks combined with their ability to approximate almost arbitrary functions with high precision allows for a new approach to this problem. Instead of evaluating the radiative transfer model itself, one can build a neural network proxy trained on the simulations but evaluating orders of magnitude faster. Such a framework is called an emulator or surrogate model. In this work, we present an emulator for the TARDIS supernova radiative transfer code applied to Type Ia supernova spectra. We show that we can train an emulator for this problem given a modest training set of a hundred thousand spectra (easily calculable on modern supercomputers). The results show an accuracy on the percent level (that are dominated by the Monte Carlo nature of TARDIS and not the emulator) with a speedup of several orders of magnitude. This method has a much broader set of applications and is not limited to the presented problem.

Keywords: methods: numerical — techniques: spectroscopic — radiative transfer

1. INTRODUCTION

Supernova spectra arise from a complex interplay of processes. Simulating them self-consistently is a computationally intensive endeavour ranging from single simulations taking several CPU minutes to thousands of CPU hours on large supercomputers.

The TARDIS (Kerzendorf & Sim 2014) supernova spectrum synthesis code can evaluate a single parametrized

explosion model within ≈ 10 CPU minutes with some approximations that have a minor impact on the output. One of the goals of TARDIS is to perform a Bayesian parameter inference on spectral time series. However, even for a very simple model for a single supernova spectrum with a fixed density profile and ten uniform abundances this results in a dozen parameters. Such parameter spaces require millions of evaluations for parameter searches which is infeasible even for fast codes like TARDIS.

Emulators are a solution to this problem (see Czekala et al. 2015, for an early implementation of emulators). These constructs approximate simulations by us-

ing functions that are easy to fit to a grid of simulations and are fast to evaluate. Lietzau (2017) did attempt to emulate TARDIS using Principal Component Analysis (PCA) and Gaussian Process (GP) regression. Lietzau (2017)’s emulator worked on eleven abundances for Type Ia supernova (SN Ia) simulations with TARDIS but was not able to work on the full set of thirteen parameters. Vogl et al. (2020) showed that using PCA and GP emulator technique worked for the lower (five) dimensional space of Type IIP supernova (SN IIP) spectra.

Neural Networks have been shown to be universal function approximators (Cybenko 1989; Hornik et al. 1989). TARDIS can be seen as a function that takes an input vector of parameters and transforms these into a spectral vector. We emulate an equivalent parameter space (our parameter space taking nuclear decay into account) to the work of (Lietzau 2017) using neural networks.

In Section 2, we describe the methods used in this emulation attempt. Section 3 summarizes the performance of the emulator (accuracy and computational efficiency). We conclude the paper in Section 4 and give an outlook of future work.

2. METHODS

The aim of the proposed emulator is to explore the posterior of Type Ia supernova spectra at roughly ten days before maximum using a uniform model for the abundances. We varied the abundances of 9 elements, one isotope, the velocity of the inner boundary, and temperature of the inner boundary (see Kerzendorf & Sim 2014, for a description of these parameters). All other parameters of the model remain fixed. We chose the density profile `branch85_w7` (a powerlaw density profile; see Kerzendorf & Sim 2014, for details) and an outer boundary velocity of $20\,000\text{ km s}^{-1}$. The plasma calculation used the `nebular` setting for ionization and `dilute-lte` setting for excitation. We use the formal integral calculated spectrum for our emulation purposes (see <https://tardis-sn.github.io/tardis/physics/montecarlo/sourceintegration.html>). The input TARDIS configuration file is available in the data cache linked to this paper <https://tinyurl.com/y77gokrr>.

There are several steps to construct an emulator for TARDIS: 1) Selecting the training set of parameters covering the necessary parameters for the specific problem. 2) Calculating the TARDIS spectra for the training set. 3) Constructing a neural network architecture. 4) Training the neural network architecture.

2.1. Data set

We are trying to use a parameter space that is close to physically realistic values. SN 2002bo is one of the

most well studied SNe Ia (309 results in ADS). Stehle et al. (2005) have done a detailed abundance tomography on this object, and Kerzendorf (2011) used this object for initial automated fitting attempts, which are a pre-cursor to the work presented here. The assumptions made in TARDIS make it most accurate before maximum and we will focus on 8.9 days after explosion (roughly ten days before maximum). We divide the creation of the training set into finding suitable abundance combinations and finding suitable inner boundary velocity and temperature combinations.

Stehle et al. (2005) model the spectrum at $8.9d$ after explosion using $v_{\text{inner}} = 13\,900\text{ km s}^{-1}$ and $T_{\text{inner}} = 11\,850\text{ K}$. We construct a uniformly spaced training grid with inner boundary temperatures (T_{inner}) between $10\,000\text{--}14\,000\text{ K}$ and inner velocities (v_{inner}) between $10\,000\text{--}15\,000\text{ km/s}$. This grid safely contains the accepted values of the parameters presented in Stehle et al. (2005).

We rely on theoretical nucleosynthesis calculations given in the Heidelberg Supernova Model Archive (HESMA; <https://hesma.h-its.org>) to find physically viable abundances. We use 62 spherically averaged isotopic models (presented in the following papers; Pakmor et al. 2010; Fink et al. 2010; Sim et al. 2010; Kromer et al. 2010; Pakmor et al. 2012; Sim et al. 2012; Röpke et al. 2012; Seitenzahl et al. 2013; Kromer et al. 2013a; Summa et al. 2013; Sim et al. 2013; Kromer et al. 2013b; Fink et al. 2014; Ohlmann et al. 2014; Kromer et al. 2015; Marquardt et al. 2015; Seitenzahl et al. 2016; Kromer et al. 2016; Noebauer et al. 2017; Fink et al. 2018) for the creation of the training set (the online data <https://tinyurl.com/y77gokrr> contains the specific list of models). We only use abundances that are in cells with velocities above $10\,000\text{ km/s}$ to be self-consistent with our choice of inner boundary velocities.

The training set is created with the abundances of O, C, Mg, Si, S, Ca, Ti, Cr, Fe (stable), and ^{56}Ni . We then calculate the location of the 20% and 80% quantile for each element excluding oxygen. We sample uniformly in \log_{10} -space between these two quantiles for all elements. Finally, we set the oxygen abundance to the remaining part of the abundance fraction.

We removed any combination of these parameters that would lead to an input luminosity of less than $1 \times 10^{42}\text{ erg s}^{-1}$. The extent of the training parameter set can be seen in Table 2.1.

We experimented with several choices of number of packets for each Monte Carlo iteration and gauged the variation for the spectrum creation resulting from the Monte Carlo nature of TARDIS (see Kerzendorf & Sim 2014, for details of this process). The choice of $100\,000$

	C	O	Mg	Si	S	Ca	Ti	Cr	Fe	⁵⁶ Ni
min	6.6e-06	0.05	2.5e-05	0.031	0.012	0.0016	3.6e-06	0.00019	0.005	0.025
25%	8.6e-05	0.51	0.00014	0.056	0.022	0.003	6.7e-06	0.00031	0.011	0.052
50%	0.0011	0.63	0.00071	0.1	0.04	0.0055	1.2e-05	0.00049	0.023	0.11
75%	0.013	0.73	0.0038	0.19	0.071	0.01	2.2e-05	0.00078	0.05	0.22
max	0.16	0.92	0.021	0.34	0.13	0.018	4.1e-05	0.0012	0.11	0.46

Table 1. The distributions of elemental abundances (uniformly in \log_{10} -space) for the training set. The two additional parameters have uniform distributions: $T_{\text{inner}} = 10000 - 14000$ K and $v_{\text{inner}} = 10000 - 15000$ km s⁻¹.

Monte Carlo packets for each iteration (opting for 30 iterations in total and increasing the number to 200 000 packets for the last iteration) resulted in spectra that had less than 1% intrinsic noise—far lower than the systematic uncertainties present in the comparison between data and spectra.

We calculated a training/validation data set with 98 000 samples and a test set with 19 930 samples on the MSU high-performance cluster provided by the Institute for Cyber-Enabled Research.

We resampled the spectra from TARDIS on a logarithmic grid between 3400 and 7600 to make the line structures across the spectrum have roughly equal pixels per structure. The final data set has 12 input parameters and 500 spectral data points. The input TARDIS file, parameters (abundances, inner boundary velocity/temperature), and spectra are available at <https://tinyurl.com/y77gokrr>.

2.2. Neural network architecture & training

We split the group of 98 000 spectra into a set of 68 600 (=70%) for training the neural networks and 29 400 for cross-validation. Each data point consisted of 12 inputs (the ‘parameters’) and 500 outputs (the ‘spectra’). Both input and output values were preprocessed by first taking the \log_{10} of the values, after which the values were normalised by removing the mean and scaling to unit variance with STANDARDSCALER (SCIKIT-LEARN; Pedregosa et al. 2011).

We use feed-forward neural networks to efficiently approximate and generalize these data. Even though training a neural network may cost a few hours of computation time, inference with trained neural networks is very fast since it only involves a small number—for the architectures used in this paper in the order of 10^6 —of floating-point operations and a few hundred nonlinear function evaluations.

We trained a number of feed-forward neural networks of different topology on the data. The neural networks were implemented in KERAS on TENSORFLOW 1.14 or 2.0.

parameter	values
# hidden layers	2–6
# neurons/layer	100–500 in steps of 100
batch size	100, 500, 1000, 2000
activation function	tanh, relu, selu, elu, softplus
optimiser	adam, nadam, adadelta, adagrad
dropout rate	0–0.6 in steps of 0.2
batch normalisation	after each layer / not at all
initialiser	glorot_normal, he_normal

Table 2. A short explanation of the hyperparameters. Activation functions: tanh is a known mathematical function which keeps the output of the neuron between +1 and -1; relu (‘rectified linear unit’) equals $\text{relu}(x) \equiv \max(0, x)$. softplus is a smooth version of relu and defined as $\ln(1 + \exp(x))$. The selu function is a normalized relu (Klambauer et al. 2017). The elu (Clevert et al. 2016) goes negative with $a(\exp(x) - 1)$ for $x < 0$.

adadelta (Zeiler 2012), adagrad (Duchi et al. 2011), adam (Kingma & Ba 2015) are modern second-order optimisation methods used in neural network training. nadam is adam but with Nesterov gradients (Sutskever et al. 2013).

Batch normalization (Ioffe & Szegedy 2015) normalises the activations of a layer of neurons per batch and helps much in preventing overfitting.

Dropout (Hinton et al. 2012) prevents overfitting by randomly switching hidden units off during training by the given rate. We never combined batch normalization with dropout. Early stopping is always done, by selecting that step in the optimization that has a low error on the cross-validation set.

Good neural network architectures were found by hyperparameter search. We used cluster-based hyperparameter search using Polyaxon 0.5.6 (<https://polyaxon.com/>) on a cluster of IBM and Nvidia machines, each with multiple Tesla V100 GPUs. Training a single neural network lasts 4–7 hours on such an architecture, and we parallelized over 200 instances.

Table 2 lists the hyperparameters over which we searched, and their range of possible values.

We chose to train the network for 15 000 epochs for networks trained without dropout and 40 000 epochs with dropout. Both numbers were chosen with a con-

siderable margin. From the approximately 4000 runs we selected the best results by analyzing their average loss (using mean squared error) over the cross-validation data set. The best found neural network architectures had a width of 200 to 400 neurons in one or two hidden layers, a softplus activation function, and Nesterov-adam as optimizer. Dropout never improved the results; batch normalization was not among the best 10 but in the best 50 networks (7% worse). As activation function softplus was in the top 30, but the difference in error with neural networks with elu, relu, selu, or tanh activations functions was not more than about 3%. The used batch size had little influence, nor did the choice of initializer.

depth	optimizer	activation	width
4	nadam	softplus	200
4	adam	softplus	200
3	adam	softplus	300
3	nadam	softplus	400
4	nadam	softplus	200

Table 3. List of five best neural network architectures used in the ensemble training.

We then selected the best neural networks for ensemble modeling (Opitz & Maclin 1999). The selected network architectures, those with the lowest loss on the cross-validation data, are listed in Table 3. Ensemble modeling was done by averaging over all listed neural networks.

3. RESULTS

In the following, we used the predictions of the ensemble neural network when comparing with the TARDIS spectra from the test set (unless otherwise noted). We used both the maximum fractional error and mean fractional error metrics (see also Vogl et al. 2020) for comparisons:

$$\text{MeanFE} = \frac{1}{N} \sum_{i=0}^N \frac{|f_{\lambda,i}^{\text{emu}} - f_{\lambda,i}^{\text{test}}|}{f_{\lambda,i}^{\text{test}}} \quad (1)$$

$$\text{MaxFE} = \max_{i=0}^N \frac{|f_{\lambda,i}^{\text{emu}} - f_{\lambda,i}^{\text{test}}|}{f_{\lambda,i}^{\text{test}}} \quad (2)$$

with N being the number of pixels in our spectra (in our case 500), $f_{\lambda,i}$ the flux at the i -th pixel in the test set. For the training of the emulator we chose to use spectra in \log_{10} . However, for the evaluation of the emulator, we will use the linear space as any likelihood comparing the emulated spectrum to an observed spectrum will be in linear flux units.

The ensemble neural network emulator performs well in both metrics with 99% of predictions having a $\text{MaxFE} < 0.049$ and $\text{MeanFE} < 0.014$ and a median prediction of $\text{MaxFE} = 0.016$ and $\text{MeanFE} = 0.004$. Figure 1 shows the best and worst prediction in the test set including residuals.

Figure 2 shows the distribution and also compares the prediction uncertainty to the networks that make up the ensemble. The ensemble has roughly a 10% improvement in MeanFE over the individual networks.

We remind the reader that TARDIS is based on an iterative Monte Carlo algorithm. The method results in variations in the final spectrum given different random seeds. We have run the worst predicting parameter set (see Figure 1) with 100 different seeds to test the variation. Figure 3 shows that the prediction uncertainty of the emulator is close to the uncertainty of the Monte Carlo algorithm.

For the desired application both MeanFE and MaxFE of the emulation will not contribute significantly as the systematic uncertainties will be much larger (MeanFE for SN 2002bo 18%; see Figure 5.5; Kerzendorf 2011).

The main reason to use an emulator compared to TARDIS itself is the speedup. The mean and standard deviation runtime for all TARDIS runs during training set creation on a single CPU on the MSU HPCC cluster are $602\text{ s} \pm 186\text{ s}$ with a minimum of 253 s and a maximum of 2054 s. Ensemble network evaluation takes $85 \pm 13.7\text{ ms}$, which is several thousand times faster than the TARDIS evaluation. A toy example of exploring likelihoods shows that a 20-dimensional problem needs 26 million evaluations (see algorithm radfriends in Table 1 in Buchner 2016), which with the emulator is possible within ≈ 25 days but not achievable without an emulator (≈ 420 years). This can be improved by forgoing ensemble modeling and taking a 10% accuracy loss but having an evaluation time of $13.3 \pm 0.46\text{ ms}$, which would do the exploration within ≈ 4 days.

4. CONCLUSION AND FUTURE WORK

We present a 12-dimensional emulator for the TARDIS radiative transfer code. The emulator can predict the spectrum with an accuracy of on average 1% with a speedup of almost 10 000 in so-called ensemble mode and a speedup of almost 50 000 with a marginally lower accuracy in single mode. A major part of the prediction uncertainty is likely not the emulator itself but noise from the Monte Carlo method of TARDIS. The chosen parameter space is focused on the SNe Ia modeling. However, the general methodology can be applied to a much broader set of problems.

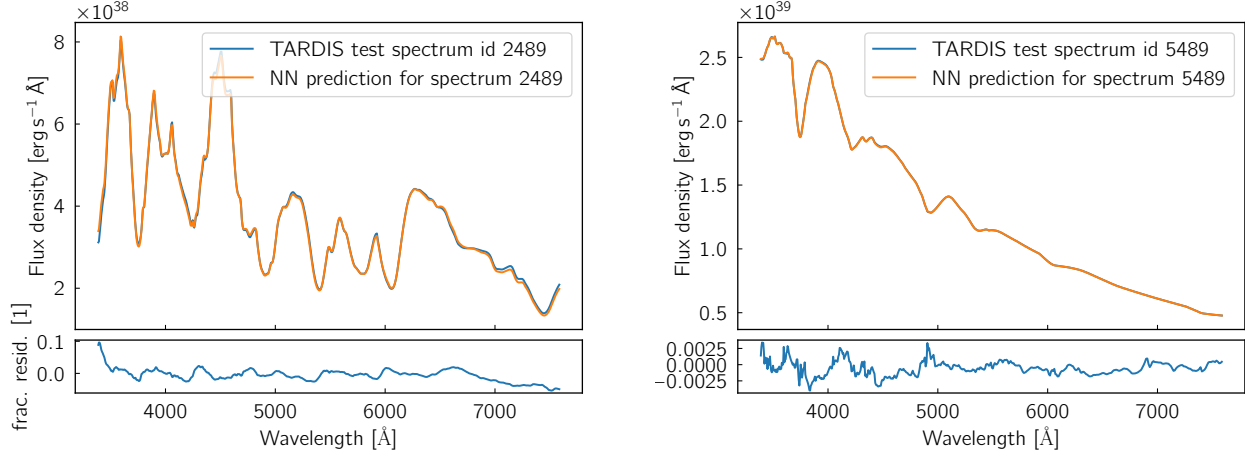


Figure 1. Comparison of a spectrum from the test set with a prediction from the ensemble emulator. We showcase the spectra with the highest and the lowest MaxFE from the set of test set predictions. **Left:** Largest MaxFE from the test set ($\approx 10\%$). **Right:** Smallest MaxFE from the test set ($\approx 0.4\%$)

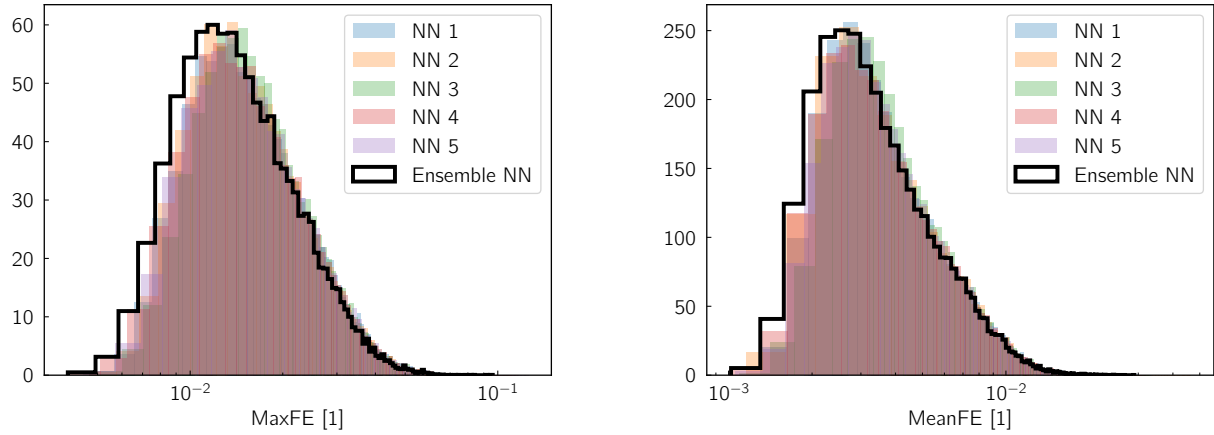


Figure 2. Histogram of prediction uncertainties for the test set using the MaxFE metric on the left and the MeanFE metric on the right.

The presented emulator is useful for exploring single spectra with abundances that are uniform throughout the envelope. Initial fitting of supernova spectra including researching likelihoods that incorporate systematic uncertainties to account for the mismatch between TARDIS and observed spectra is already underway.

A complete reconstruction of an exploded object from spectral time series will have more than a hundred parameters. This will require the development of more complex emulators. For such parameter spaces, we will need to use more constraining priors when generating the training set. The authors have already experimented with various schemes to find a training set (e.g., drawing from Kernel Density estimates of the HESMA abundances) but such work is outside the current scope of

exploring neural networks as function approximators for radiative transfer codes.

We have shown that emulators enable the exploration of high-dimensional parameter spaces even with costly simulations. Such tools will be important assets for the data-rich era that astronomy is entering.

CONTRIBUTOR ROLES

We use the CRT standard (see <https://casrai.org/credit/>) for reporting our contributor roles:

- **Conceptualization** - Kerzendorf, Vogl
- **Data curation** - Kerzendorf
- **Formal Analysis** - Kerzendorf, PvdS

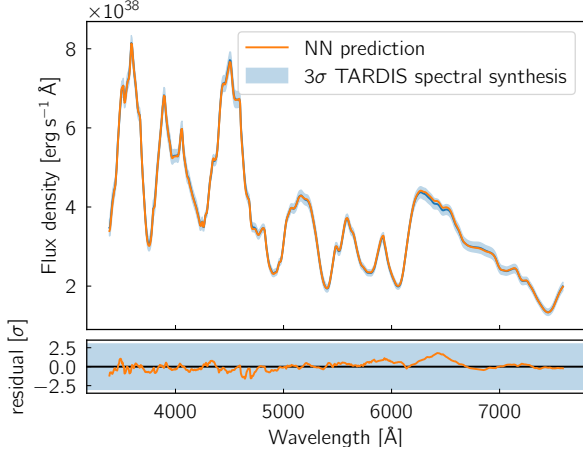


Figure 3. Comparison of the emulator prediction uncertainty with the Monte Carlo uncertainty.

- **Investigation** - Kerzendorf, PvdS, Contardo, Buchner
- **Methodology** - Kerzendorf, PvdS
- **Resources** - PvdS, Kerzendorf

- **Software** - Kerzendorf, PvdS, Vogl, Williamson
- **Validation** - Kerzendorf, PvdS
- **Visualization** - Kerzendorf, PvdS
- **Writing—original draft** - Kerzendorf, PvdS
- **Writing—review & editing** - Kerzendorf, PvdS, Vogl, Williamson, Contardo, Buchner

ACKNOWLEDGEMENTS

This research made use of TARDIS, a community-developed software package for spectral synthesis in supernovae (Kerzendorf & Sim 2014; Vogl et al. 2019; Kerzendorf et al. 2020). The development of TARDIS received support from the Google Summer of Code initiative and from ESA’s Summer of Code in Space program. TARDIS makes extensive use of Astropy and PyNE.

This work was supported in part through computational resources and services provided by the Institute for Cyber-Enabled Research at Michigan State University. Neural network training was done at Volkswagen Group. This work made use of the Heidelberg Supernova Model Archive (HESMA), <https://hesma.h-its.org>.

The authors would like to thank Gabriella Contardo for helpful with learning the neural network

REFERENCES

- Buchner, J. 2016, *Statistics and Computing*, 26, 383, doi: [10.1007/s11222-014-9512-y](https://doi.org/10.1007/s11222-014-9512-y)
- Clevert, D.-A., Unterthiner, T., & Hochreiter, S. 2016, in *Proc. Int. Conf. on Learning Representations (ICLR)*. <https://arxiv.org/abs/1511.07289>
- Cybenko, G. 1989, *Mathematics of Control, Signals and Systems*, 2, 303
- Czekala, I., Andrews, S. M., Mandel, K. S., Hogg, D. W., & Green, G. M. 2015, *ApJ*, 812, 128, doi: [10.1088/0004-637X/812/2/128](https://doi.org/10.1088/0004-637X/812/2/128)
- Duchi, J., Hazan, E., & Singer, Y. 2011, *Journal of Machine Learning Research*, 12, 2121. <http://jmlr.org/papers/v12/duchi11a.html>
- Fink, M., Kromer, M., Hillebrandt, W., et al. 2018, *A&A*, 618, A124, doi: [10.1051/0004-6361/201833475](https://doi.org/10.1051/0004-6361/201833475)
- Fink, M., Röpke, F. K., Hillebrandt, W., et al. 2010, *A&A*, 514, A53, doi: [10.1051/0004-6361/200913892](https://doi.org/10.1051/0004-6361/200913892)
- Fink, M., Kromer, M., Seitzzahl, I. R., et al. 2014, *MNRAS*, 438, 1762, doi: [10.1093/mnras/stt2315](https://doi.org/10.1093/mnras/stt2315)
- Hinton, G. E., Srivastava, N., Krizhevsky, A., Sutskever, I., & Salakhutdinov, R. R. 2012, *Improving neural networks by preventing co-adaptation of feature detectors*. <https://arxiv.org/abs/1207.0580>
- Hornik, K., Stinchcombe, M., & White, H. 1989, *Neural Networks*, 2, 359, doi: [https://doi.org/10.1016/0893-6080\(89\)90020-8](https://doi.org/10.1016/0893-6080(89)90020-8)
- Ioffe, S., & Szegedy, C. 2015, *Batch Normalization: Accelerating Deep Network Training by Reducing Internal Covariate Shift*. <https://arxiv.org/abs/1502.03167>
- Kerzendorf, W., Sim, S., Vogl, C., et al. 2020, *tardis-sn/tardis: TARDIS v3.0.dev3463, v3.0.dev3463*, Zenodo, doi: [10.5281/zenodo.3902923](https://doi.org/10.5281/zenodo.3902923)
- Kerzendorf, W. E. 2011, PhD thesis, Australian National University, Research School of Astronomy & Astrophysics
- Kerzendorf, W. E., & Sim, S. A. 2014, *MNRAS*, 440, 387, doi: [10.1093/mnras/stu055](https://doi.org/10.1093/mnras/stu055)
- Kingma, D. P., & Ba, J. 2015, in *International Conference on Learning Representations*. <https://arxiv.org/abs/1412.6980>
- Klambauer, G., Unterthiner, T., Mayr, A., & Hochreiter, S. 2017, in *Advances in Neural Information Processing Systems* 30, Vol. abs/1706.02515. <https://arxiv.org/abs/1706.02515>
- Kromer, M., Sim, S. A., Fink, M., et al. 2010, *ApJ*, 719, 1067, doi: [10.1088/0004-637X/719/2/1067](https://doi.org/10.1088/0004-637X/719/2/1067)

- Kromer, M., Fink, M., Stanishev, V., et al. 2013a, MNRAS, 429, 2287, doi: [10.1093/mnras/sts498](https://doi.org/10.1093/mnras/sts498)
- Kromer, M., Pakmor, R., Taubenberger, S., et al. 2013b, ApJL, 778, L18, doi: [10.1088/2041-8205/778/1/L18](https://doi.org/10.1088/2041-8205/778/1/L18)
- Kromer, M., Ohlmann, S. T., Pakmor, R., et al. 2015, MNRAS, 450, 3045, doi: [10.1093/mnras/stv886](https://doi.org/10.1093/mnras/stv886)
- Kromer, M., Fremling, C., Pakmor, R., et al. 2016, MNRAS, 459, 4428, doi: [10.1093/mnras/stw962](https://doi.org/10.1093/mnras/stw962)
- Lietzau, S. 2017, Master’s thesis, Technical University Munich, doi: [10.5281/zenodo.1312512](https://doi.org/10.5281/zenodo.1312512)
- Marquardt, K. S., Sim, S. A., Ruiter, A. J., et al. 2015, A&A, 580, A118, doi: [10.1051/0004-6361/201525761](https://doi.org/10.1051/0004-6361/201525761)
- Noebauer, U. M., Kromer, M., Taubenberger, S., et al. 2017, MNRAS, 472, 2787, doi: [10.1093/mnras/stx2093](https://doi.org/10.1093/mnras/stx2093)
- Ohlmann, S. T., Kromer, M., Fink, M., et al. 2014, A&A, 572, A57, doi: [10.1051/0004-6361/201423924](https://doi.org/10.1051/0004-6361/201423924)
- Opitz, D., & Maclin, R. 1999, Journal of artificial intelligence research, 11, 169
- Pakmor, R., Kromer, M., Röpke, F. K., et al. 2010, Nature, 463, 61, doi: [10.1038/nature08642](https://doi.org/10.1038/nature08642)
- Pakmor, R., Kromer, M., Taubenberger, S., et al. 2012, ApJL, 747, L10, doi: [10.1088/2041-8205/747/1/L10](https://doi.org/10.1088/2041-8205/747/1/L10)
- Pedregosa, F., Varoquaux, G., Gramfort, A., et al. 2011, Journal of Machine Learning Research, 12, 2825
- Röpke, F. K., Kromer, M., Seitzzahl, I. R., et al. 2012, ApJL, 750, L19, doi: [10.1088/2041-8205/750/1/L19](https://doi.org/10.1088/2041-8205/750/1/L19)
- Seitzzahl, I. R., Ciaraldi-Schoolmann, F., Röpke, F. K., et al. 2013, MNRAS, 429, 1156, doi: [10.1093/mnras/sts402](https://doi.org/10.1093/mnras/sts402)
- Seitzzahl, I. R., Kromer, M., Ohlmann, S. T., et al. 2016, A&A, 592, A57, doi: [10.1051/0004-6361/201527251](https://doi.org/10.1051/0004-6361/201527251)
- Sim, S. A., Fink, M., Kromer, M., et al. 2012, MNRAS, 420, 3003, doi: [10.1111/j.1365-2966.2011.20162.x](https://doi.org/10.1111/j.1365-2966.2011.20162.x)
- Sim, S. A., Röpke, F. K., Hillebrandt, W., et al. 2010, ApJL, 714, L52, doi: [10.1088/2041-8205/714/1/L52](https://doi.org/10.1088/2041-8205/714/1/L52)
- Sim, S. A., Seitzzahl, I. R., Kromer, M., et al. 2013, MNRAS, 436, 333, doi: [10.1093/mnras/stt1574](https://doi.org/10.1093/mnras/stt1574)
- Stehle, M., Mazzali, P. A., Benetti, S., & Hillebrandt, W. 2005, MNRAS, 360, 1231, doi: [10.1111/j.1365-2966.2005.09116.x](https://doi.org/10.1111/j.1365-2966.2005.09116.x)
- Summa, A., Ulyanov, A., Kromer, M., et al. 2013, A&A, 554, A67, doi: [10.1051/0004-6361/201220972](https://doi.org/10.1051/0004-6361/201220972)
- Sutskever, I., Martens, J., Dahl, G., & Hinton, G. 2013, in International conference on machine learning, 1139–1147
- Vogl, C., Kerzendorf, W. E., Sim, S. A., et al. 2020, A&A, 633, A88, doi: [10.1051/0004-6361/201936137](https://doi.org/10.1051/0004-6361/201936137)
- Vogl, C., Sim, S. A., Noebauer, U. M., Kerzendorf, W. E., & Hillebrandt, W. 2019, A&A, 621, A29, doi: [10.1051/0004-6361/201833701](https://doi.org/10.1051/0004-6361/201833701)
- Zeiler, M. D. 2012, ADADELTA: An Adaptive Learning Rate Method. <https://arxiv.org/abs/1212.5701>